New insights into the kinetics of metal|electrolyte interphase growth in solid-state-batteries via an *operando* XPS analysis - part I: experiments

Edouard Quérel,[1,*] Nicholas J. Williams,[1] Ieuan D. Seymour,[1] Stephen J. Skinner,[1] Ainara Aguadero,[1,3]

[1]Department of Materials, Imperial College London, Exhibition Road, London, SW7 2AZ, UK

[2] Instituto de Ciencia de Materiales de Madrid, ICMM-CSIC, Sor Juana Ines de La Cruz 3, 28049, Madrid, Spain

*Correspondence: edouard_querel@hotmail.com

ABSTRACT

To harness all the benefits of solid-state battery (SSB) architectures in terms of energy density, their negative electrode should be an alkali metal. However, the high chemical potential of alkali metals make them prone to reduce most solid electrolytes (SE), resulting in a decomposition layer called an *interphase* at the metal|SE interface. Quantitative information about the interphase chemical composition and rate of formation are challenging to obtain because the reaction occurs at a buried interface.

In this study, a thin layer of Na metal (Na^0) is plated on the surface of a SE of the NaSICON family ($Na_{3.4}Zr_2Si_{2.4}P_{0.6}O_{12}$ or NZSP) inside a commercial XPS system whilst continuously analysing the composition of the interphase *operando*. We identify the existence of an interphase at the Na^0|NZSP interface, and more importantly, we demonstrate for the first time that this protocol can be used to study the kinetics of interphase formation.

A second important outcome of this article is that the surface chemistry of NZSP samples can be tuned to improve their stability against Na^0. It is demonstrated by XPS and time-resolved electrochemical impedance spectroscopy (EIS) that a native Na_3PO_4 layer present on the surface of as-sintered NZSP samples protects their surface against decomposition.

Keywords: NaSICON, Na metal, electrochemical stability, SEI, interphase, operando XPS, plasmons

INTRODUCTION

Among the avenues considered to improve the performance and safety of Li-ion batteries, the elimination of hazardous liquid electrolytes and their replacement by solid electrolytes (SEs) in cell architectures called solid-state-batteries (SSBs) provides an attractive option.[1] Indeed, if employing high-capacity alkali metal negative electrodes, SSBs offer a solution to simultaneously increase the energy density, power density and safety of cells. Whilst it was initially believed that SSBs would also benefit from an intrinsic long-term stability,[2] it has later been demonstrated that the lifetime of SSBs is highly impacted by degradation at the electrode|SE interface. Some of these issues are related to the electrochemical stability of the SE with regards to electrode materials and the formation of interphases upon decomposition of the SE. This initial instability is not necessarily an issue if a stable solid electrolyte interphase (SEI) can be formed, such as at

the interface between graphite and optimized liquid electrolytes in conventional Li-ion cells.[3] The decomposition of the SE against an alkali metal leads to the formation of interphases whose electronic properties will dictate its growth:[4] (a) if a majority of the decomposition products are electronically insulating, the growth of the SEI will eventually stop and if it does not form a large barrier to ionic migration, its impact on the power performance of a cell may be tolerable or (b) if the decomposition products are electronically conducting, the growth of the mixed ionic electronic conducting (MIEC) interphase will be uninterrupted until all the SE is consumed and a short-circuit occurs. This latter interphase type is not compatible for SSB with long-lasting performance. Having access to the chemical composition of the interphase is essential in determining which type of interphase is produced and whether stability will be reached in a cell.

X-ray photoelectron spectroscopy (XPS) is an excellent surface characterization technique for chemical composition analysis. Analyzing the composition of a buried interface is however a challenge because of the limited depth resolution of XPS. The limited depth resolution of XPS is due to the nature of the measurement which relies on the collection of photoelectrons which escape from a sample surface after travelling a short distance away from the atomic nucleus they initially bounded with (typically within a depth of less than 10 nm for photoelectrons excited by an Al Kα source and travelling through Na metal). Recently, a variety of *in-situ* [5–7] and *operando* techniques [8,9] have been developed to address this problem. For all of them, the idea is to make the alkali metal layer on the surface of the SE thin enough to let photoelectrons emitted by the SE (and possibly by interphases) go through the metal overlayer. To produce the alkali metal layer, one technique consists of plating it on the surface of the SE from a counter electrode composed of the same alkali metal whilst analysing the interphase products *in-operando*.[8] What enables the plating in that case is the provision of low energy electrons to the surface of the SE from the electron flood gun present in any XPS instrument. Whilst this technique has already proven its efficacy at characterizing the composition of interphases, the extent of information which can be extracted from it (such as the growth rate behaviour of the alkali metal layer) has not yet been fully appreciated. The objective of this study is to present the depth of information which can be extracted from this *operando* protocol. The results are separated into two paired articles (part I: experiment; and part II: theory).

In part 1, the plating of Na metal (Na^0) on the surface of a sodium conducting SE of the NaSICON family ($Na_{3.4}Zr_2Si_{2.4}P_{0.6}O_{12}$, further referred to as NZSP) is studied. NZSP was chosen for this study because of its good electrochemical performance that makes it a promising candidate SE,[10] but its stability against Na^0 is still debated. Theoretical DFT calculations predict that $Na_3Zr_2Si_2PO_{12}$ (the closest phase on the convex hull of the NaSICON compositional space defined by $Na_{1+x}Zr_2Si_xP_{3-x}O_{12}$, $0 \leq x \leq 3$) is unstable at 0 V against Na/Na^+ and should form an interphase composed of Na_2ZrO_3, Na_4SiO_4, Na_3P, and ZrSi.[11–13] The formation of a stable SEI at the Na^0| $Na_3Zr_2Si_2PO_{12}$ was also suggested experimentally by electrochemical impedance spectroscopy and *ex-situ* XPS studies.[13,14]

This study will distinguish two types of Na^0|NZSP interfaces: the first is the interface between Na^0 and a polished NZSP ($NZPS_{polished}$) pellet; the second is the interface between Na^0 and an as-sintered NZSP ($NZSP_{AS}$) pellet. This comparison is intended to clarify the impact of the NZSP surface chemistry on its stability against Na^0. Indeed, it was identified in a previous study from our group that thermal treatments promote the formation of a thin Na_3PO_4 layer on the surface of as-sintered NZSP samples, a layer which was removed when the NZSP surface was polished.[10] As Na_3PO_4 is a phase which is predicted to be stable against Na^0 by DFT calculations,[12] the aim of this comparison is to evaluate the efficiency of Na_3PO_4 as a self-formed buffer layer.

The discussion of this first experimental part focuses on extracting information from the XPS fitting models to inform on the kinetics of interphase formation at both the Na^0|$NZSP_{polished}$ and Na^0|$NZSP_{AS}$ interfaces. Time resolved electrochemical impedance spectroscopy (EIS) is also employed to evaluate the ionic resistivity of the interphases.

This experimental study is accompanied by a theoretical study (part 2) where it is demonstrated that information extracted from the XPS fitting models can be used to validate the coupled ion-electron transfer (CIET) theory.

EXPERIMENTAL SECTION

NZSP synthesis

$Na_{3.4}Zr_2Si_{2.4}P_{0.6}O_{12}$ powders were synthesized following a solution-assisted solid-state synthesis described in a previous publication.[10] Pellet samples were produced from this mother powder and sintered in Pt crucibles (1285 °C, 6h, 180 °C h^{-1} heating and cooling rates).

After sintering, the pellets which are hereinafter referred to as "as sintered" (or $NZSP_{AS}$) were quickly transferred to an Ar filled glovebox for storage without further treatment to their surface. The pellets which are referred to as "polished" ($NZSP_{polished}$) were polished with 500 grit SiC paper using ethanol as lubricating solvent, sonicated in ethanol for one minute, and then transferred to a glovebox for storage.

X-ray photoelectron spectroscopy (XPS)

The Na^0|NZSP half-cells used for the *operando* plating experiment were assembled inside an Ar filled glovebox (O_2 and H_2O levels below 1 ppm). Circular Na^0 counter electrodes were punched from a freshly prepared Na^0 foil for each new half-cell (Na metal rod, 99%, Alfa Aesar). The surface of the Na^0 electrode was mechanically cleaned using the blade of a scalpel before being pressed against one side of the NZSP pellet. This Na^0|NZSP half-cell was transferred to the XPS instrument (Thermo Fisher Scientific K-Alpha XPS system) using a vacuum transfer vessel (Thermo Fisher Scientific XPS Vacuum Transfer Module).

XPS spectra were collected at room temperature with a monochromated Al K_α source (1486.6 eV) operating at a power of 72 W (6 mA x 12 kV). The analysis area is an ellipsoid of dimensions *ca.* 400 µm x 800 µm. As described in the introduction, the charge compensating flood gun (FG) of the instrument was diverted from its intended use and employed to supply electrons for the Na^0 plating reaction on the NZSP surface. A specificity of this instrument is that charge compensation relies on a dual mode flood source (electrons and Ar^+ ions) which are not independently controlled. A recent publication demonstrated that the bombardment of the interface by Ar^+ ions during plating can impact the interphase composition.[15] To minimize the Ar^+ ion flux reaching the interface, the extractor voltage of the instrument was reduced to 30 V following the results of a previous study.[16] The Na^0 plating rate was controlled by optimizing the FG parameters: the beam voltage was set to 3 V, and the current was set to 30 µA (the actual electronic current reaching the sample surface was measured using a Faraday cup and a value of ~4.8 µA was found; the Ar^+ current reaching the surface is ~10 nA).The base pressure of the instrument (FG off) is typically around 1 x 10^{-9} mbar and rises to around 1 x 10^{-8} mbar when the FG is activated. The change in pressure is related to the introduction of a small volume of Ar gas in the analysis chamber associated with the design of the dual mode flood source.
Core level spectra were measured using a pass energy of 20 eV, at a resolution of 0.1 eV and an integration time of 50 ms/point. A compromise between the speed of acquisition and the quality of the data had to be determined: short iterations are required because the continuous plating of Na^0 leads to a rapid attenuation of the interface signals; but iterations should be long enough to detect chemical shifts in low intensity signals. The adequate FG current was found empirically by testing different currents; it should be high enough for the plating reaction to occur (X-rays generate holes and shift the equilibrium of the plating reaction).

XPS fitting

All spectra were fitted using the algorithms implemented in the CasaXPS software. Shirley backgrounds were employed for all core level signals with minimal inelastic backgrounds (*i.e.* Zr 3d, Si 2p, P 2p). For Na 1s regions, plasmon resonances produce a significant inelastic background and a three parameter Tougaard background function was employed (U 4 Tougaard: B,33,0.8,0) where the intensity of the parameter B was adapted for each fit.

Most peaks were fitted using a symmetric LA(1.53,243) line shape (a Voigt function). This line shape cannot be used to model the Na metal peak which has a tail on the high binding energy (BE) side of the peak. An exact procedure to model asymmetric peaks in XPS is still debated.[17] The only asymmetric peak shape with a theoretical basis is the Doniach-Sunjic (DS) one. However, a problem with the DS function is that its asymptotic form means it integrates to infinity. The extracted peak area is therefore dependent on the defined energy region. In a recent review, Major *et al.* propose a series of solutions to address the asymmetry problem, including the use of finite Lorentzian (LF) functions to overcome the problem of non-integrability of the DS function.[17] For the main Na metal peak, a LF(0.58,1.17,200,80) line shape was employed.

Cell assembly and electrochemical impedance spectroscopy (EIS)

Na metal films were freshly prepared for each assembled cell in an Ar-filled glovebox. A clean piece of Na^0 was cut (Na cubes, 99.9%, Sigma Aldrich), then pressed flat in a LDPE plastic bag to a thickness of ~150 µm. Circular electrodes were then punched from this foil. Their surface was mechanically cleaned using the blade of a scalpel. The Na metal electrodes were then placed on both sides of a NZSP pellet and the Na|NZSP|Na stack was pressed with a uniaxial pressure of around 10 MPa. The symmetrical cells were then placed in 2032 type coin cells. Battery grade Al foil was used as a non-alloying current collector between the Na^0 electrode and stainless steel casing.

Impedance spectra were measured on a Biologic VMP-300 potentiostat with an excitation amplitude of $V_{A.C.}$ = 50 mV in the frequency range of 7 MHz-5Hz, with a 20 cycles integration period at each frequency and a 1 cycle delay after each frequency jump. Results were fitted using RelaxIS3 (Rhd instruments).

RESULTS

Operando plating of Na^0 on NZSP surfaces

The working principle of the *operando* plating of Na^0 on the NZSP using the flood gun of an XPS instrument is schematically represented in Figure 1a. The results presented in this section were obtained with a polished NZSP sample ($NZSP_{polished}$).

The analysis sequence starts with the FG initially turned off. A first set of survey and core level spectra are measured and constitute a reference for the bare NZSP surface prior to any plating or SEI formation (shown in red in Figure 1). The FG is then turned on and core level spectra are measured over 4 hours in an iterative loop with each acquisition cycle (*i.e.* one set of Na 1s, Zr 3d, P 2p, Si 2p, O 1s and C 1s core level data) lasting 18 minutes and 11 seconds. The successive sets of XPS spectra are presented in Figure 1 in shades of blue, from light blue for the first cycle (0 h of plating) to dark blue for the last cycle (around 4 h of plating).

A qualitative description of Figure 1 reveals that: (1) Na^0 was successfully plated on the surface of NZSP using the FG; this is indicated by the growth of an intense XPS peak at 1071.8 eV (whose attribution to Na^0 will be detailed later); (2) several new peaks appear in the Na 1s and O 1s core level regions as plating progresses; (3) the intensity of the Zr 3d, P 2p, Si 2p, and C 1s signals decreases as plating progresses which confirms that an overlayer is growing on top of NZSP; (4) a change in the shape of the Zr 3d signal with a tail to lower binding energies in comparison to the reference sample is observed as plating progresses; (5) the rate at which the Na metal peak grows is rapid in the first cycles and slows down subsequently; (6) all core level spectra experience a shift to lower binding energy between the flood gun off and flood gun on condition; (7) a continuous shift to lower binding energies (BE) of the peak referenced as Na NZSP and Na Auger is observed in the Na 1s and O 1s core level regions.

To construct a physically meaningful surface model to fit the XPS data from Figure 1, the XPS signature of Na metal needs to be isolated first. For this purpose, a XPS analysis of a pristine Na metal foil was conducted.

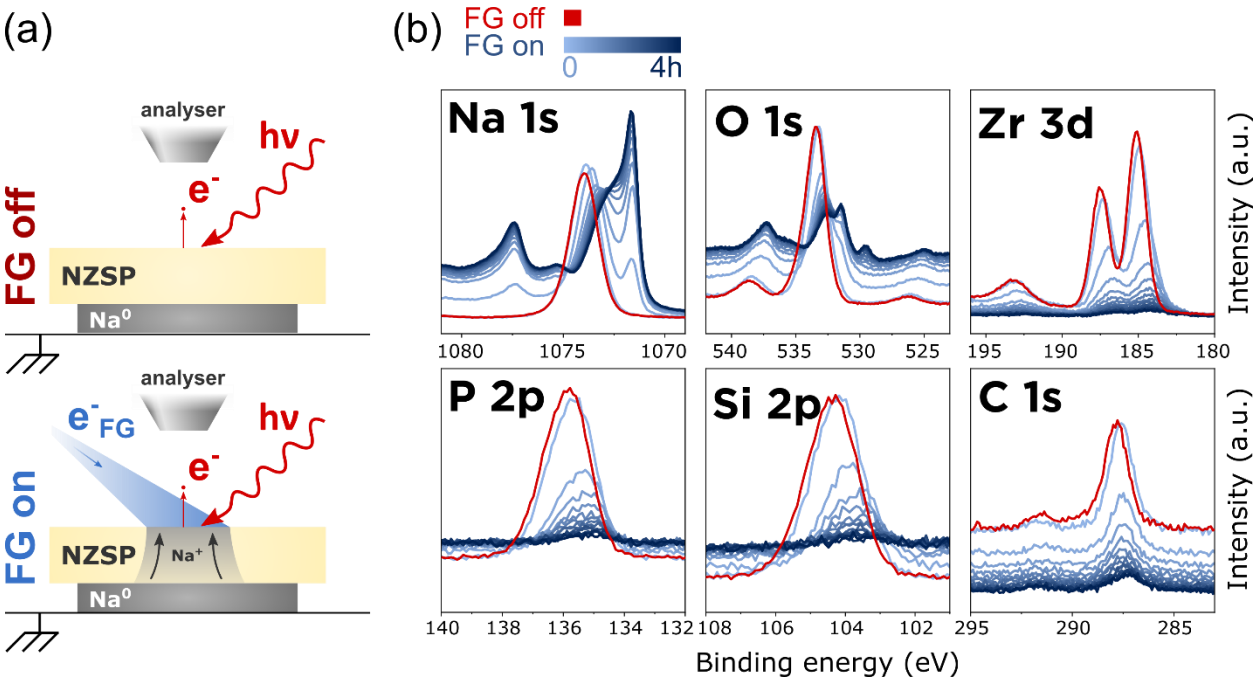

Figure 1. Demonstration of the working principle of the *operando* plating of Na^0 inside the XPS. (a) Schematic representation of the two XPS analysis configurations: when the FG is off, the chemical composition of the bare NZSP surface is analyzed; when the FG is on, Na^0 can plate on the top surface of NZSP and the changes in chemical composition are monitored *in-operando*; (b) Evolution of selected core level regions with increasing Na^0 plating time. An initial set of data (in red) was measured with the FG off (reference signal from $NZSP_{polished}$). The following spectra (in shades of blue) were measured in an iterative loop (each iteration lasted 18 minutes and 11 seconds).

XPS signature of pristine Na^0

The XPS signature of Na metal was obtained by analyzing separately the surface of a Na metal sample (99 %, Alfa Aesar). The sample was prepared inside an Ar filled glovebox and transferred to the XPS instrument via a vacuum transfer vessel. Despite having taken such precautions, a passivation layer was found on the surface of the sample (see Figure S1). To remove the passivation layer, the Na metal foil was sputter cleaned using a 2 keV Ar^+ ion gun for a total sputtering time of 3 hours. The removal of surface contaminants was confirmed in the survey spectrum by the disappearance of the signals in the O-KLL and C 1s regions and by the metallic Fermi edge in the valence band region.

Figure 2 shows XPS signals of the Na 1s and “O 1s” regions of the sputter cleaned Na metal sample. The Na 1s region was scanned over a wide BE range, Figure 2(a), to collect multiple plasmon peaks. Figure 2(b) provides a narrower range view of the Na 1s region centered around the main Na^0 peak. Figure 2(c) shows the XPS signals in the region where O 1s signals are typically found (between 520 and 545 eV). The region is called the “O 1s” region in relation to Figure 1 but it should be noted that the peaks are primarily caused by Na metal Auger photoelectrons and their plasmon losses.

Figure 2(a) shows that the main Na^0 peak (at 1071.83 eV) is followed by a series of periodic plasmon peaks. A plasmon is a collective oscillation of the valence electrons of a metallic sample.[18] The peaks which appear periodically at higher BE from the main Na^0 peak are photoelectrons which have lost one or several quanta of energy to excite plasmon resonances. Photoemission can excite bulk and surface plasmons in metallic samples. In Figure 2(a), bulk plasmons produce strong peaks at integral multiples of ΔE_{BP} = 5.85 eV from the main Na^0 peak. The first surface plasmon is observed at ΔE_{SP} = 3.97 eV from the main Na^0 peak (the experimental ratio ΔE_{BP}/ ΔE_{SP} = 1.47 is close to the theoretical value of $\sqrt{2}$). Other surface plasmons are observed at multiples n. ΔE_{BP}+ΔE_{SP} (with n, an integer number) which corresponds to the case when a photoelectron excites n bulk plasmons and a surface plasmon as it exits to the surface of the sample.

Barrie and Street analyzed the XPS signals of sodium metal and sodium oxide in 1975 but a fitting model for the Na 1s region of Na^0 and its inelastic background are, to the best of our knowledge, not available in the literature.[19] Because plasmon resonances introduce a strong modification of the inelastic background up to 50 eV below the main peak, appropriate peak fitting requires the use of a Tougaard background instead of the more common Shirley option.[20] The Tougaard background function was parameterized from the wide region XPS scan (Figure 2(a)): the function replicates the periodicity of the bulk plasmon losses and the background reaches the baseline at 30 eV higher BE from the main peak. Figure 2(a)) shows that the Tougaard function models the intensity of the background well away from the main peak (at 15 eV higher BE upwards), but that it underestimates the intensity of the first and second plasmon peaks. This is because the Tougaard function employed does not model intrinsic plasmons only extrinsic ones.[21,22] Intrinsic plasmons are excited at the photoemission site and simultaneously to the photoemission event whereas extrinsicplasmons are excited away from the photoemission site as photoelectrons travel through the metal Figure 2(d) schematically represents the difference between intrinsic and extrinsic plasmons. In this work, the contribution from intrinsic plasmons was modelled using separate peaks indicated in Figure 2(b). It is important to note that these peaks are part of the inelastic background of the Na^0 peak and are not primary photoelectrons. Figure 2(b) also shows that the main asymmetric Na^0 peak was modelled using a finite Lorentzian (LF) function. A LF function was preferred over a Doniach Sunjic function to limit the tail of the metal peak and enable the integration of its area without introducing a cutoff.[17] The fitting model parameters are presented in Table S1.

Figure 2(c) provides an identification of the peaks in the “O 1s” region. The most intense peak at 531.6 eV is a Na-$KL_1L_{2,3}$ Auger peak. It is important to notice that the position of this Auger peak differs between metallic sodium and sodium oxides.[19] For instance, the Na-$KL_1L_{2,3}$ Auger from NZSP is located at 7.3 eV higher binding energies (around 538.9 eV in Figure 1). Auger photoelectrons can also excite plasmons and the plasmon peaks are observed with the same periodicity as in the Na 1s region (at multiples of ΔE_{BP}=5.8 eV and ΔE_{SP}=3.97 eV). The peak observed at 525 eV is the second plasmon peak of Na-$KL_{2,3}L_{2,3}$ Auger photoelectrons.

To assess the reactivity of Na metal with residual gases inside the XPS chamber, the Na metal foil was left for 6 hours under ultra-high vacuum ($5x10^{-9}$ mbar) with all guns off (X-ray, sputter, charge compensation). The XPS survey and core level signals of the Na metal sample after the 6 hours pause are presented in Figures S1 and S2. The Na 1s and O 1s signals clearly indicate the formation of a passivation layer on the Na^0 surface. Thus, even under ultra-high vacuum conditions, a passivation layer can form on the surface of Na metal films in a few hours. It is important to note that the *operando* metal plating experiment (Figure 1) typically lasts around 4 hours which leaves enough time for a passivation layer to form on the surface of the plated Na metal.

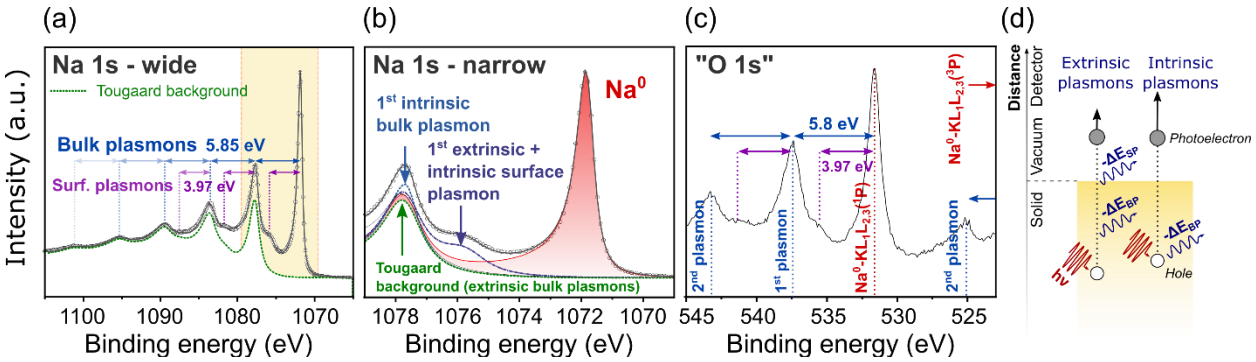

Figure 2. Fitting model of sputter-cleaned Na metal. (a) Na 1s region measured over a wide BE range. The yellow box indicates the region which is magnified in panel (b); (b) Fitting model of the Na 1s region. Several peaks were added to model the background.(c) Identification of the peaks observed in the "O 1s" region. (d) Schematic showing different origins of plasmon excitations.

Fitting model for the $Na^0|NZSP_{polished}$ interface

The Na metal fitting model previously established is used in this section as a reference to identify the new peaks which appeared during the *operando* plating of Na^0 on top of $NZSP_{polished}$ (experiment described in Figure 1). As the most significant changes affected the Na 1s, O 1s, and Zr 3d signals, these core levels were modelled in Figure 3. Figure 3 compares the XPS signals of three samples: the $Na^0|NZSP_{polished}$ interface after 91 minutes of plating, the reference sputter-cleaned Na^0 surface, and a reference $NZSP_{polished}$ surface.

Na 1s: The Na 1s region of $Na^0|NZSP_{polished}$ is constituted of five peaks. Three of these peaks correspond to the Na 1s signature of Na^0 (see Figure 2) and can therefore be assigned to the freshly plated Na^0 layer: the most intense peak is the asymmetric Na^0 peak at 1071.9 eV (in red in Figure 3); it is followed by the first surface and bulk plasmon peaks respectively at 3.96 eV and 5.86 eV higher BE from the Na^0 peak (in dashed lines). As a reminder, these plasmon peaks are part of the Na^0 peak background and are not produced by a separate phase. In addition to these three Na^0 peaks, the feature observed between 1073 and 1074 eV was separated into two peaks corresponding to photoelectrons emitted by the NZSP phase (in orange) and by the interphase and/or a surface passivation layer (in purple). The area of the NZSP peak was constrained to respect the stoichiometry (Na:Si ratio) of the reference data (in red). Details on the fitting strategy which permitted the separation of the NZSP and interphase peaks can be found in the Supplementary Information. The full list of fitting constraints and calculated parameters can be found in Tables S2 and S3.

O 1s: The O 1s region of the $Na^0|NZSP_{polished}$ interface was only qualitatively compared with that of $NZSP_{polished}$ and Na^0 in Figure 3 because of the large number of overlapping peaks in this region. The peaks observed in the 523-545 eV range of the $Na^0|NZSP_{polished}$ interface are produced by: (i) Na-KLL Auger electrons from the plated Na^0 layer, from the NZSP phase and from the newly formed interphase and passivation layer; (ii) plasmon peaks; (iii) O 1s photoelectrons from the NZSP phase and from the interphase and passivation layer.

Zr 3d: the fitting model for the Zr 3d region of the $Na^0|NZSP_{polished}$ interface consists of three doublets. The first of these doublets (in blue) corresponds to Zr 3d photoelectrons emitted by the NZSP phase. A tail appears in the 181-184 eV region as soon as Na^0 plating starts which suggests that an interphase forms. The additional doublets required to fit the tail were constrained to have the same FWHM as that of the

NZSP doublet. It was found that two doublets were required to obtain a fitting model with low residuals. The chemical composition of the phases giving rise to these signals could not be unambiguously determined with this experiment. Thus, the new doublets are referred to as “int.1” and “int.2” (for “interphase 1/2”) in Figure 3. Future work will be required to confirm if one of these doublets can be assigned to Na_2ZrO_3 which is one of the decomposition products predicted to form at the $Na^0|Na_3Zr_2Si_2PO_{12}$ interface from first principles calculations.[11–13] In addition to Na_2ZrO_3, ZrSi and ZrP are two other phases predicted to form at the $Na^0|Na_3Zr_2Si_2PO_{12}$ interface by DFT. It is however unlikely that the interphase doublets correspond to these phases because their formation would result in a clear signal in the Si 2p and P 2p regions which was not observed (see below).

Si 2p and P 2p: The formation of an interphase at the $Na^0|NZSP_{polished}$ interface did not result in significant changes of the Si 2p and P 2p signals (see Figure S3). As previously mentioned, the formation of Na_3P, ZrSi, and ZrP could not be detected although these phases are predicted to form by DFT. Because P is in a (-III) oxidation state in Na_3P and ZrP and Si is in a (-IV) oxidation state in ZrSi, the presence of any of these phases should result in a peak at lower BE in comparison to the NZSP peaks (where P is in a (+V) state and Si is in a (+IV) state).

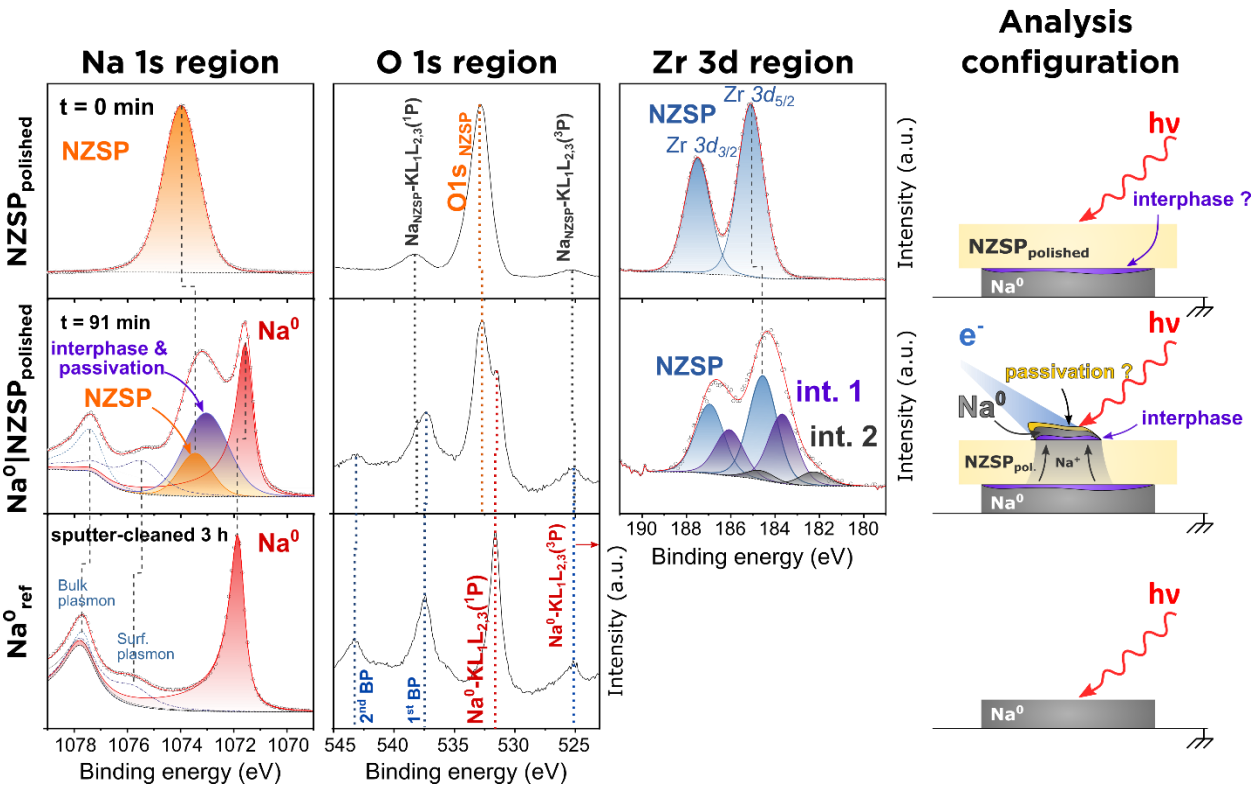

Figure 3 – Fitting model for the $Na^0|NZSP_{polished}$ interface. Fitting parameters and constraints are listed in Tables S2 and S3.

Fitting model for the $Na^0|NZSP_{AS}$ interface and role of Na_3PO_4 as a protecting layer

The results from the previous section established that polished NZSP pellets form an interphase in contact with Na metal. This section investigates the stability of as-sintered NZSP pellets against Na^0. As a reminder, it was established in a previous study that the surface of $NZSP_{AS}$ samples is terminated by a thin Na_3PO_4 layer.[10] The aim of this section is therefore to clarify whether this layer has an impact on the stability of NZSP against Na^0.

The same procedure was employed to plate Na^0 on the surface of a $NZSP_{AS}$ pellet (see Figure S4). Figure 4 shows the fitting model for the Na 1s and Zr 3d core levels of a $Na^0|NZSP_{AS}$ interface after 240 minutes of Na^0 plating (also included on the figure are the XPS signature of reference $NZSP_{AS}$ and Na^0 surfaces). A distortion of the Zr 3d signal is clearly observed after the initiation of plating at the $Na^0|NZSP_{AS}$ interface. New peaks corresponding to the new interphase species are included in the fitting model in Figure 4, but the ratio of the interphase signals to the NZSP signal is much smaller than for the $Na^0|NZSP_{polished}$ interface, which indicates that the interphase is thinner when Na^0 is in contact with $NZSP_{AS}$ than with $NZSP_{polished}$. No significant changes in the shape of the Si 2p and P 2p signals were observed for $Na^0|NZSP_{AS}$ in comparison to $NZSP_{AS}$ (Figure S5). The relative shift in peak positions are analyzed in the Discussion and in Part II of this study.

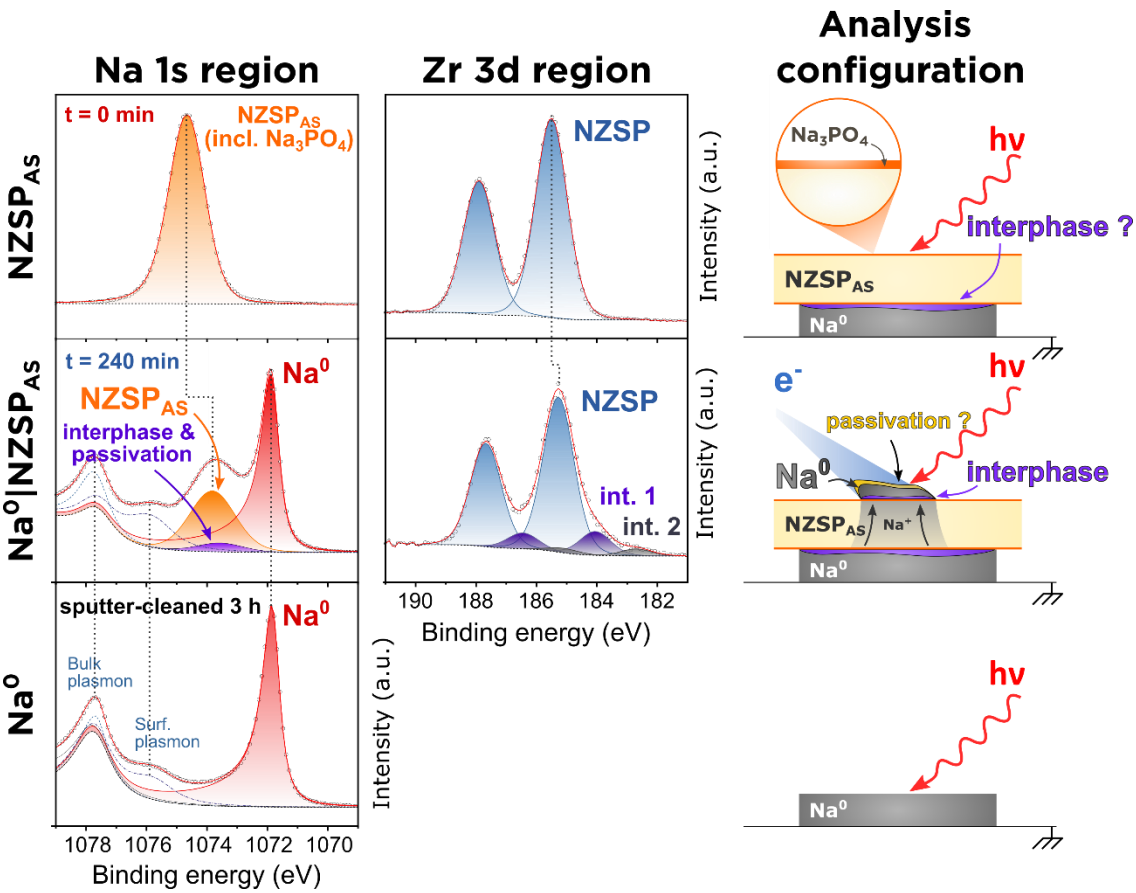

Figure 4 – Fitting model for the Na^0|$NZSP_{AS}$ interface. The dataset for the Na^0|$NZSP_{AS}$ interface is that obtained after 240 minutes of Na^0 plating. Fitting parameters and constraints are listed in Tables S4 and S5.

Evolution of the peak areas as a function of plating time

Figure 5(a) and (b) plot the relative evolution of peak areas as Na^0 plating progresses. The peaks were individually normalized relative to their maximum area over the course of the experiment. The moment when this maximum is reached differs depending on the peak: for instance, the Na^0 peak reaches its maximum at the end of the experiment (*i.e.* when the plated Na^0 layer is the thickest), whereas the peaks corresponding to NZSP are most intense at the beginning of the experiment (before NZSP gets covered by an overlayer). For both the Na^0|$NZSP_{AS}$ and Na^0|$NZSP_{polished}$ interfaces, the growth of the Na^0 peak can be separated into two regions: a fast initial growth (in the first 100 minutes of plating) after which the rate of plating slows down.

The formation of an interphase at both the Na^0|$NZSP_{AS}$ and Na^0|$NZSP_{polished}$ interfaces was detected by the appearance of new species in the Zr 3d signals in Figures 3 and 4. The evolution of the normalized relative area of one of these peaks ("int. 1") is included in Figure 5(a) and (b) (in purple). Figure 5(a) shows that the normalized area of the "int. 1" peak attenuates as plating progresses which indicates that Na^0 grows on top of the "int. 1" phase. The normalized relative area of the "int. 1" peak is larger than the NZSP peaks (*e.g.* Zr 3d) which also suggests that the new phase lies on top of the NZSP phase. In contrast, for the Na^0|$NZSP_{polished}$ interface, the intensity of the "int. 1" peak initially increases in the first minutes of Na^0 plating before attenuating. The rate at which the "int. 1" peak attenuates is also slower than that of the NZSP peaks. This suggests that the decomposition of NZSP and the formation of an interphase occurs over a longer time with a polished pellet than with an as sintered one. The ratio of the Zr 3d signal emitted by the interphase products to the total Zr 3d signal (%interphase) was also plotted in Figure 5 (black stars) with:

$$\%interphase = \frac{A_{int.1}^{Zr3d_{5/2}} + A_{int.2}^{Zr3d_{5/2}}}{A_{NZSP}^{Zr3d_{5/2}} + A_{int.1}^{Zr3d_{5/2}} + A_{int.2}^{Zr3d_{5/2}}}$$

where $A_{int.1}^{Zr3d_{5/2}}$, $A_{int.2}^{Zr3d_{5/2}}$, and $A_{NZSP}^{Zr3d_{5/2}}$ correspond to the area of the Zr $3d_{5/2}$ peaks of the interphase 1, interphase 2 and NZSP phases in the peak fitting models used in Figures 3 and 4.

This ratio provides information about the progression of the decomposition reaction occurring at the interface. The decomposition reaction takes around 2 hours to stabilize for the Na^0|$NZSP_{polished}$ interface whereas it is almost immediate for the Na^0|$NZSP_{AS}$ interface. The fraction of the Zr 3d signal emitted by the interphase is around 15 % for the Na^0|$NZSP_{AS}$ interface and up to 60 % for the Na^0|$NZSP_{polished}$ interface. $NZSP_{polished}$ surfaces therefore decompose to a much greater extent than $NZSP_{AS}$ surfaces in contact with Na^0.

The main conclusion of this sub-section is that the NZSP surface chemistry influences its stability versus Na^0. $NZSP_{AS}$ samples (whose surface is terminated by a thin Na_3PO_4 layer) are more stable in contact with Na^0 than $NZSP_{polished}$. The Na_3PO_4 layer acts as a protecting layer preventing the formation of a thick interphase. Another important conclusion is that for both Na^0|$NZSP_{AS}$ and Na^0|$NZSP_{polished}$, the decomposition reaction eventually stabilizes which suggests that the reaction products are electronically insulating and form a self-limiting SEI-type interphase.[23] The formation of a self-limiting interphase is crucial to ensure the long-term stability of Na^0|NZSP based batteries.

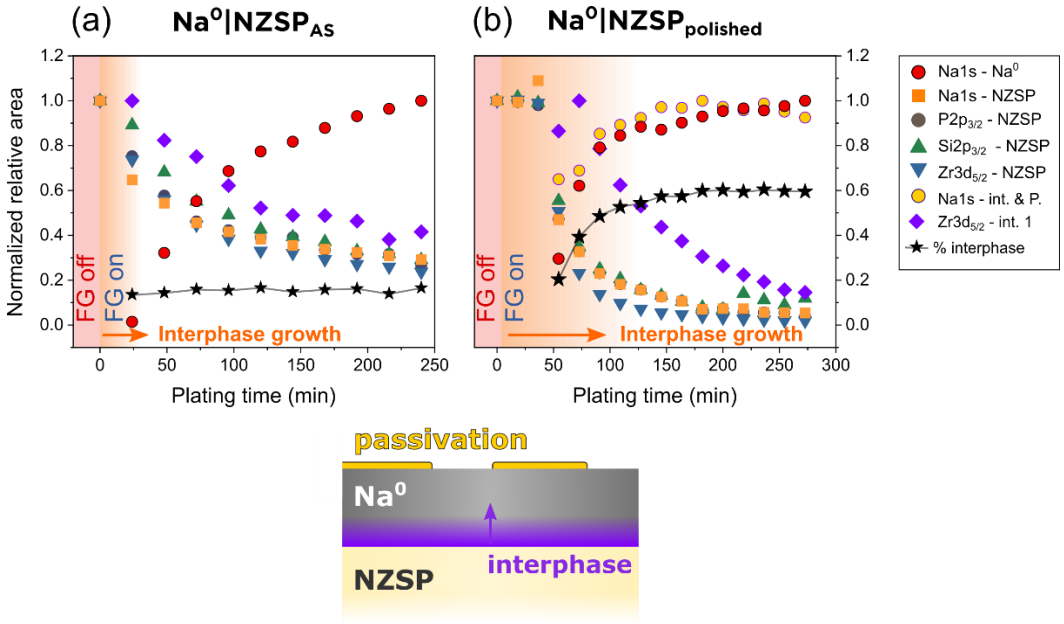

Figure 5 – Evolution of the fitting model peak areas as a function of plating time. (a) Fitted peak areas (normalized to their relative maximum) as a function of plating time for the $Na^0|NZSP_{AS}$, and (b) for the $Na^0|NZSP_{polished}$ interface. A schematic cross-section of the proposed interface model is included below the graphs.

Relative shifts of the peak positions as a function of plating time

Figure 6(a) and (b) show the relative shifts in the positions of peaks as plating progresses for the $Na^0|NZSP_{AS}$ and $Na^0|NZSP_{polished}$ interfaces. For NZSP photoelectrons, the shifts are calculated with respect to the peak position measured in the reference (FG off) experiment. The peak position is affected by the surface potential that the photoelectrons experience as they escape the surface into vacuum. In other words, if a surface potential accelerates photoelectrons when they leave the surface, the resulting peak will appear in the spectrum at a lower BE than it would normally appear without the surface potential. The surface potential is continuously changing in the *operando* experiment from the combined effect of Na^0 plating and the formation of an interphase. Thus, it is not surprising to observe a shift in the position of peaks in Figure 6. For the $Na^0|NZSP_{AS}$ interface (Figure 6(a)), an initial shift of all of the peaks happens in the first few minutes of plating but the peaks then stop shifting for the rest of the experiment. The relative shifts of the Na 1s and P 2p peaks are more pronounced (-0.6 to -0.8 eV) than the Si 2p or Zr 3d peaks (around -0.2 eV). The more pronounced shift of the Na 1s and P 2p peaks is attributed to the presence of some thicker Na_3PO_4 "islands" on the surface of $NZSP_{AS}$ (Figure S6) leading locally to a larger surface potential. For the $Na^0|NZSP_{polished}$ interface (Figure 6(b)), the position of the peaks is seen to continuously shift in the first 90 minutes of plating before reaching more stable values.

The Si 2p and P 2p peak positions begin to shift after 150 minutes of plating (sometimes by more than 0.2 eV between two consecutive iterations). This scatter is a fitting artefact which is caused by the difficulty in extracting a precise position for the peaks when their intensity is too low. The continuous shift of the peaks in the first 90 minutes of plating indicates that a surface potential is building up. This growing surface potential can be attributed to the growing thickness of the interphase. In other words, the evolution of the peak positions confirms that the interphase forms over a longer period for the $Na^0|NZSP_{polished}$ interface in comparison to the $Na^0|NZSP_{AS}$ interface.

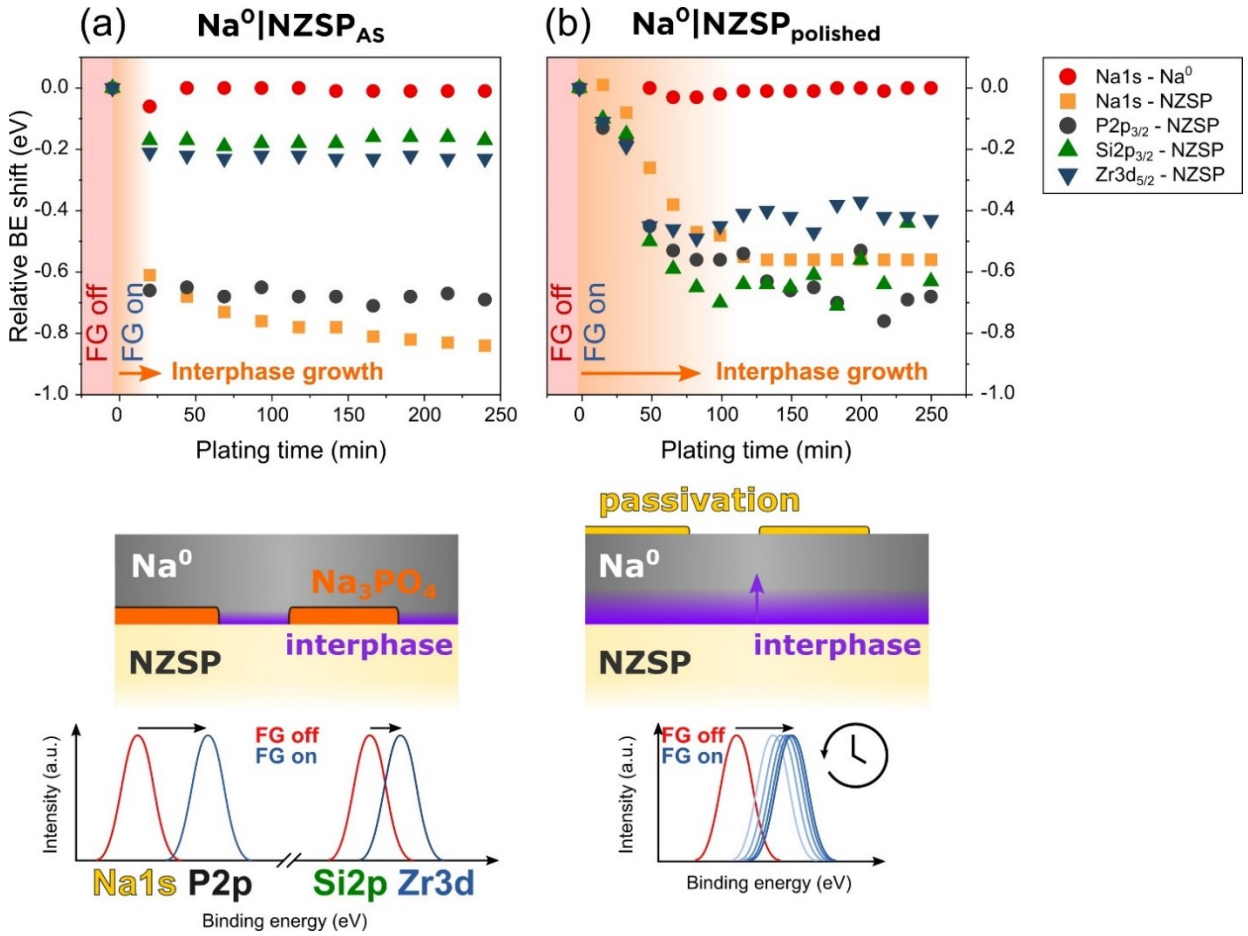

Figure 6 – Relative shifts in peak positions as a function of plating time for the $Na^0|NZSP_{AS}$ interface (a) and the $Na^0|NZSP_{polished}$ interface (b).

Aging dynamics of $Na^0|NZSP$ interfaces by electrochemical impedance spectroscopy (EIS)

The *operando* XPS experiments established the protecting role of the thin Na_3PO_4 layer on the surface of $NZSP_{AS}$ samples against the formation of a thick SEI upon contact with Na^0. The enhanced stability against Na^0 of $NZSP_{AS}$ samples in comparison to $NZSP_{polished}$ samples is studied here by time-resolved EIS.

Two symmetrical cells consisting of a $NZSP_{AS}$ or $NZSP_{polished}$ pellet sandwiched between two Na^0 electrodes were assembled and the evolution of their impedance was monitored over a little more than one day (with a time interval Δt=1 h or 0.5 h respectively) at 25°C. The impedance of the two cells are presented in Figure 7(a) and (b) in the form of Nyquist plots. The Nyquist plots were fitted to the equivalent circuit included in inset in Figure 7(a). As established in previous studies, the high-frequency semi-circle (apex at 1.5 MHz) corresponds to grain boundary diffusion in the NZSP pellet.[10,24] The second semi-circle appearing at lower frequencies (apex at 5 kHz in Figure 7(b)) corresponds to the diffusion of Na^+ ions across the $Na^0|NZSP$ interface. The initial interface resistance of the cell assembled with $NZSP_{AS}$ is lower (0.3±0.1 Ω cm^2) than the cell assembled with $NZSP_{polished}$ (120±7 Ω cm^2). This initial difference in interface resistance just after cell assembly was studied in more detail in a previous publication from our group.[10]

Regarding the evolution of the $Na^0|NZSP$ interface resistance as a function of time, Figure 7 shows that the increase is rapid in the first hours after cell assembly before stabilizing. This aging behaviour suggests that

the interphase between Na^0 and NZSP is self-limiting, *i.e.* that the decomposition species are electronically insulating (an interphase type commonly referred to as a SEI [23]). In addition, Figure 7 shows that the decomposition more strongly affects the cell assembled with $NZSP_{polished}$ than the cell assembled with $NZSP_{AS}$. In Figure 7(c) the interface resistance of the $NZSP_{AS}$ cell increased from 0.3±0.1 Ω cm^2 to 2.0±0.1 Ω cm^2 in 24 h, whereas in Figure 7(d) the interface resistance of the $NZSP_{polished}$ cell increased from 120±7 Ω cm^2 to 360±20 Ω cm^2 in 30 h.

The EIS results indicate that $NZSP_{AS}$ samples are more stable against Na metal than $NZSP_{polished}$ samples. We attribute this to the presence of a protective Na_3PO_4 layer on the surface of $NZSP_{AS}$ samples. Overall, the XPS and EIS results are aligned and demonstrate that a thicker and more resistive SEI forms at the Na^0|$NZSP_{polished}$ interface in comparison to the Na^0|$NZSP_{AS}$ one.

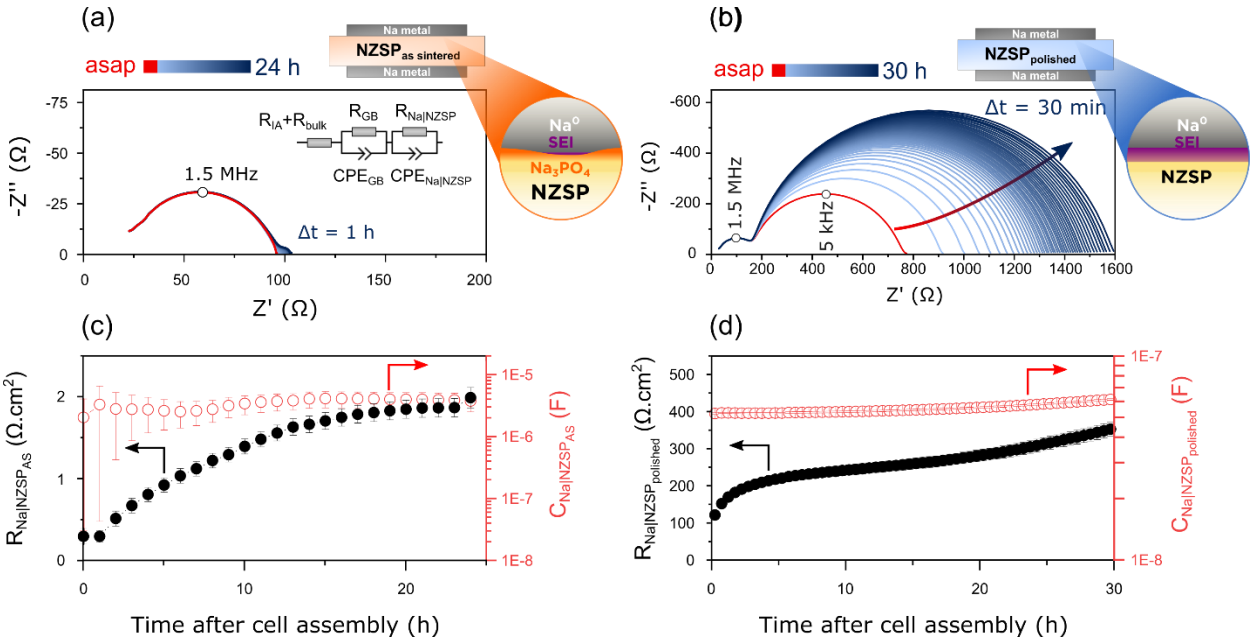

Figure 7 – Time resolved impedance spectra comparing the aging dynamics of two Na|NZSP|Na symmetrical cells assembled either with an as sintered NZSP pellet (a), or a polished NZSP pellet (b). The equivalent circuit included in inset of panel (a) was used to fit the impedance data ($R_{IA}R_{bulk}$: combined resistor accounting for the ohmic resistance of the impedance analyser and the bulk resistance of the NZSP pellet; R_{GB} and CPE_{GB}: grain boundary resistance and constant phase element; $R_{Na|NZSP}$ and $CPE_{Na|NZSP}$: Na|NZSP interface resistance and CPE). The evolution of the Na|$NZSP_{AS}$ interface resistance and capacitance as a function of time is presented in panel (c). The evolution of the Na|$NZSP_{polished}$ interface resistance and capacitance as a function of time is presented in panel (d). The cells were aged in a climate chamber at a temperature of 25°C.

CONCLUSION

Characterizing the decomposition reaction occurring at a buried interface with a technique whose depth resolution is limited to a few nanometres (such as XPS) is a challenging task. The *operando* experiment described in this study provides a lot of information in a single experiment and is therefore a very valuable tool in the characterization of alkali metal|SE interfaces. More precisely, the information which can be extracted from it includes: the detection of new phases from the decomposition reaction at the interface;

the equilibration time for the decomposition reaction; the rate of Na^0 plating on the NZSP surface; and surface potentials associated with the growth of the interphase.

The first article of this two-part study focused on establishing physically meaningful XPS fitting models for the Na^0|NZSP interface whilst Na^0 is being plated on the NZSP surface. For the Na 1s core level in particular, the models had to separate the signal emitted by the Na^0 overlayer from the signals emitted by NZSP and the SEI. In future work, the XPS signals coming from the SEI will have to be assigned to specific phases by measuring the signal of reference SEI samples. A starting point for the identification of new phases is the list of decomposition products predicted by first principles calculations, including for instance Na_2ZrO_3 or Na_4SiO_4.[12] We note that recent studies suggested that dual mode charge compensating XPS instruments (such as the one employed in this study) may alter the chemistry of the interphase because of the energy provided by the impacts from Ar^+ ions on the surface.[15] To minimize this effect, the Ar^+ ion current was reduced in this study.

One important conclusion of the study is the superior stability of thermally activated $NZSP_{AS}$ surfaces in contact with Na^0 in comparison to polished $NZSP_{polished}$ ones. This is due to the protecting nature of the Na_3PO_4 surface termination of $NZSP_{AS}$ samples. The greater stability of $NZSP_{AS}$ samples against Na^0 in comparison to $NZSP_{polished}$ was also demonstrated by time-resolved EIS.

In part II of this study, data extracted from the XPS fittings from this article are used in a CIET model to gain more detailed information about the kinetics of the plating reaction and SEI formation on $NZSP_{AS}$ and $NZSP_{polished}$ surfaces.

ACKNOWLEDGMENTS

The authors thank Dr. Gwilherm Kerherve for his help with the XPS system, and Dr. Peter Klusener for fruitful discussions as part of the collaboration with Shell. This work has been funded by the Engineering and Physical Sciences Research Council (EP/R002010/1), Shell Global Solutions International B.V., and Ceres Power Ltd.

DATA ACCESS

The XPS and EIS data and fitting models used in this work are accessible on the following Zenodo repository: 10.5281/zenodo.6672033

DECLARATION OF INTERESTS

The authors declare no competing interests.

REFERENCES

1. Janek, J. & Zeier, W. G. A solid future for battery development. *Nat. Energy* **1**, 1–4 (2016).
2. Li, J., Ma, C., Chi, M., Liang, C. & Dudney, N. J. Solid Electrolyte: the Key for High-Voltage Lithium Batteries. *Adv. Energy Mater.* **5**, 1401408 (2015).
3. Gauthier, M. *et al.* Electrode-Electrolyte Interface in Li-Ion Batteries: Current Understanding and New Insights. *Journal of Physical Chemistry Letters* **6**, 4653–4672 (2015).
4. Krauskopf, T., Richter, F. H., Zeier, W. G. & Janek, J. Physicochemical Concepts of the Lithium Metal Anode in Solid-State Batteries. *Chemical Reviews* **120**, 7745–7794 (2020).
5. Wenzel, S., Leichtweiss, T., Krüger, D., Sann, J. & Janek, J. Interphase formation on lithium solid electrolytes - An in situ approach to study interfacial reactions by photoelectron spectroscopy. *Solid*

State Ionics **278**, 98–105 (2015).

6. Wenzel, S. *et al.* Interfacial Reactivity Benchmarking of the Sodium Ion Conductors Na 3 PS 4 and Sodium β-Alumina for Protected Sodium Metal Anodes and Sodium All-Solid-State Batteries. *ACS Appl. Mater. Interfaces* **8**, 28216–28224 (2016).
7. Kehne, P. *et al.* Sc-substituted Nasicon solid electrolyte for an all-solid-state NaxCoO2/Nasicon/Na sodium model battery with stable electrochemical performance. *J. Power Sources* **409**, 86–93 (2019).
8. Wood, K. N. *et al.* Operando X-ray photoelectron spectroscopy of solid electrolyte interphase formation and evolution in Li2S-P2S5 solid-state electrolytes. *Nat. Commun.* **9**, 1–10 (2018).
9. Connell, J. G. *et al.* Kinetic versus Thermodynamic Stability of LLZO in Contact with Lithium Metal. *Chem. Mater.* **2020**, 46 (2020).
10. Querel, E. *et al.* The role of NaSICON surface chemistry in stabilizing fast-charging Na metal solid-state batteries. *J. Phys. Energy* **3**, (2021).
11. Tang, H. *et al.* Probing Solid−Solid Interfacial Reactions in All-Solid-State Sodium- Ion Batteries with First-Principles Calculations. *Chem. Mater.* **30**, 163–173 (2017).
12. Lacivita, V., Wang, Y., Bo, S. H. & Ceder, G. Ab initio investigation of the stability of electrolyte/electrode interfaces in all-solid-state Na batteries. *J. Mater. Chem. A* **7**, 8144–8155 (2019).
13. Zhang, Z. *et al.* Na3Zr2Si2PO12 : A Stable Na + -Ion Solid Electrolyte for Solid-State Batteries. *ACS Appl. Energy Mater.* **19**, 39 (2020).
14. Gao, Z. *et al.* Stabilizing Na3Zr2Si2PO12/Na Interfacial Performance by Introducing a Clean and Na-Deficient Surface. *Chem. Mater.* **32**, 3970–3979 (2020).
15. Gibson, J. *et al.* Gently Does It!: In Situ Preparation of Alkali Metal - Solid Electrolyte Interfaces for Photoelectron Spectroscopy. *Faraday Discuss.* (2022). doi:10.1039/D1FD00118C
16. Edwards, L., Mack, P. & Morgan, D. J. Recent advances in dual mode charge compensation for XPS analysis. *Surf. Interface Anal.* **51**, 925–933 (2019).
17. Major, G. H. *et al.* A discussion of approaches for fitting asymmetric signals in X-ray photoelectron spectroscopy (XPS), noting the importance of Voigt-like peak shapes. *Surf. Interface Anal.* (2021). doi:10.1002/sia.6958
18. Kittel, C. *Introduction to Solid State Physics*. (Wiley, 2005).
19. Barrie, A. & Street, F. J. An Auger and X-ray photoelectron spectroscopic study of sodium metal and sodium oxide. *J. Electron Spectros. Relat. Phenomena* **7**, 1–31 (1975).
20. Tougaard, S. Quantitative analysis of the inelastic background in surface electron spectroscopy. *Surf. Interface Anal.* **11**, 453–472 (1988).
21. Tougaard, S. Practical algorithm for background subtraction. *Surf. Sci.* **216**, 343–360 (1989).
22. Tougaard, S. Energy loss in XPS: Fundamental processes and applications for quantification, non-destructive depth profiling and 3D imaging. *J. Electron Spectros. Relat. Phenomena* **178**–**179**, 128–153 (2010).
23. Wenzel, S. *et al.* Interphase formation and degradation of charge transfer kinetics between a lithium metal anode and highly crystalline Li7P3S11 solid electrolyte. *Solid State Ionics* **286**, 24–33 (2016).
24. Ma, Q. *et al.* Room temperature demonstration of a sodium superionic conductor with grain conductivity in excess of 0.01 S cm −1 and its primary applications in symmetric battery cells. *J. Mater. Chem. A* **7**, 7766–7776 (2019).

Supplementary information

New insights into the kinetics of metal|electrolyte interphase growth in solid-state-batteries via an *operando* XPS analysis - part I: experiments

Edouard Quérel,[1,*] Nicholas Williams,[1] Ieuan D. Seymour,[1] Stephen Skinner,[1] Ainara Aguadero,[1,2]

[1]Department of Materials, Imperial College London, London, SW7 2AZ, UK

[2] Instituto de Ciencia de Materiales de Madrid, ICMM-CSIC, Sor Juana Ines de La Cruz 3, 28049, Madrid, Spain

*Correspondence: edouard_querel@hotmail.com

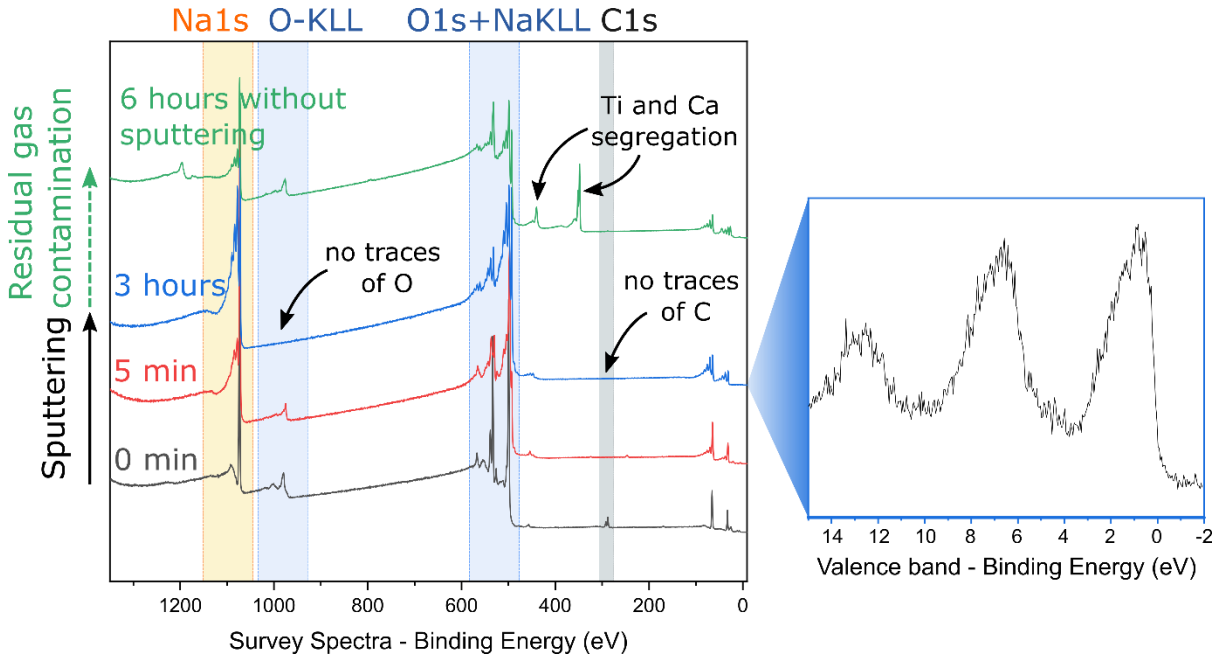

Figure S1 – Evolution of the survey spectra of a Na metal sample as a function of sputtering time. Despite having been prepared inside a clean glovebox and transferred to the XPS instrument in a vacuum transfer module, the surface of as-prepared Na metal foils (t = 0min) are passivated as indicated by the presence of C and O on the surface. Because Na-KLL photoelectrons are found in the same region as O1s photoelectrons, the O-KLL region is better to monitor the level of O contamination from the surface. Sputtering for 5 minutes is not enough to remove all traces of C and O from the surface. After 3 hours, all traces of contamination have disappeared. After that, the sample was left for 6 hours in the XPS chamber to assess the contamination from residual gases in the chamber. After 6 hours, a clear O signal is detected. The segregation of Ca and Ti (two residual species found in our 99% pure Na metal ingots) to the surface during these 6 hours is a thermodynamically driven process: reaction energies of -0.574 eV/atom and -0.375 eV/atom for the reactions $Na_2O + Ca \rightarrow CaO + 2Na$ and $Na_2O + Ti \rightarrow TiO + 2Na$ respectively were extracted from the Materials Project.[1] The slight misalignment of the valence band Fermi edge with the calibrated zero of the instrument was previously associated to the complexity of removing all contaminants on the non-sputtered side of the Na^0 foil (i.e. at the interface between the sample stage and Na^0 foil)[2]. Related to Figure 2.

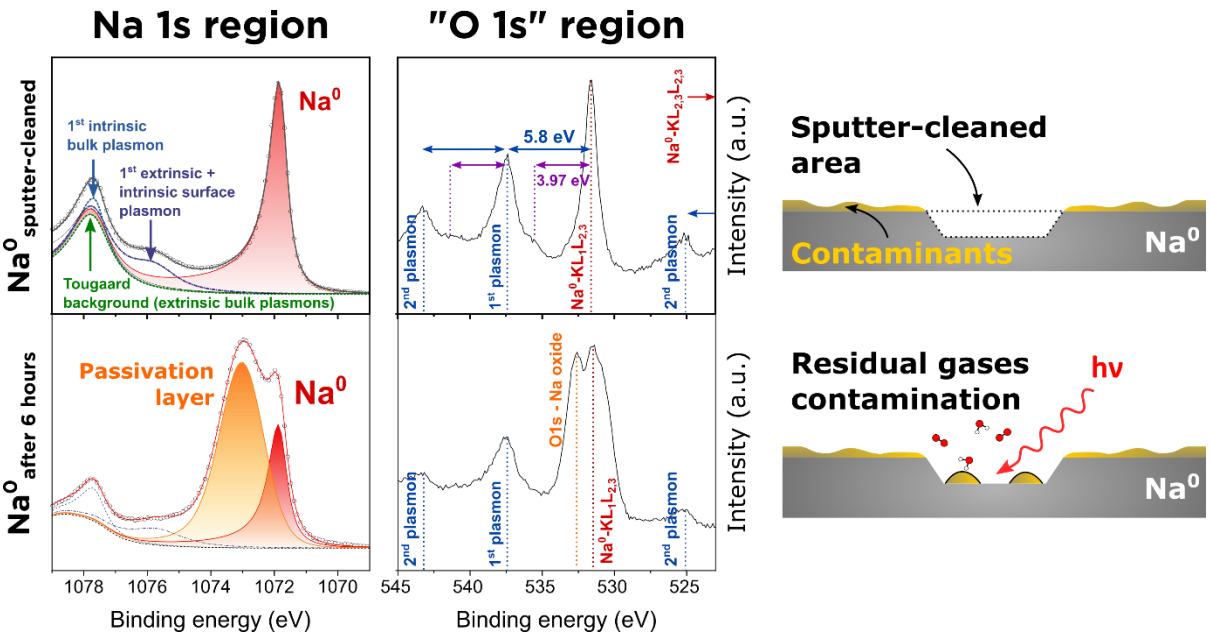

Figure S2 – Residual gas contamination of Na metal. Na1s and O1s XPS signals of a sputter-cleaned Na metal sample (top) and the same Na metal sample after 6 hours of exposure to the residual gases of the XPS chamber under ultra-high vacuum conditions. The Na1s photoelectron signal emitted by the species forming the passivation layer was modelled by a single peak with a wide FWHM. The formation of a passivation layer at the Na^0 surface is also indicated by a new peak at 532.6 eV in the O1s region. Establishing the exact composition of the passivating species which formed on the Na^0 surface was not required for this study. Related to Figure 2.

		Fitting			Constraints			
Region	Peak	BE (eV)	FWHM (eV)	Area	Line shape	BE (eV)	FWHM (eV)	Area
Na1s	Na0	1071.83	0.61	277172	LF(0.58,1.15,200,50)	1071.8 - 1071.9	<0.65	-
	1st extr.+intr. SP	1075.8	1.77	93174	//	1075.8-1075.85	-	-
	1st intr. BP	1077.61	0.59	23667	//	1077.61-1077.65	-	-
	Unidentified singlet	1079.8	2.92	100000	//	1079.8-1079.85	-	<100000
	1st extr. BP+SP	1081	3.93	18973	//	1081-1082	-	-

Table S1 – XPS fitting parameters of the sputter-cleaned Na metal sample. extr./intr. = extrinsic/intrinsic. SP = surface plasmon, BP = bulk plasmon. Related to Figure 2.

		Fitting			Constraints			
Region	Peak	BE (eV)	FWHM (eV)	Area	Line shape	BE (eV)	FWHM (eV)	Area
Na1s	NZSP	1073.94	1.59	227806	LA(1.25,1.53,243)	-	-	-
P2p	3/2 NZSP	135.66	1.36	4448	LA(1.53,243)	-	-	-
	1/2 NZSP	136.53	1.36	2224	//	P2p3/2 + 0.87	P2p3/2 *1	P2p3/2*0.5
Si2p	3/2 NZSP	104.2	1.56	3500	LA(1.53,243)	-	-	-
	1/2 NZSP	104.8	1.56	1750	//	Si2p3/2 +0.6	Si2p3/2*1	Si2p3/2*0.5
Zr3d	5/2 NZSP	185.09	1.37	22059	LA(1.53,243)	-	-	-
	3/2 NZSP	187.49	1.37	14706	//	Zr3d5/2 (NZSP) + 2.4	Zr3d5/2 (NZSP)*1	Zr3d5/2 (NZSP)*0.667

Table S2 – XPS fitting parameters of the reference $NZSP_{polished}$ sample. Related to Figure 3.

		Fitting			Constraints			
Region	Peak	BE (eV)	FWHM (eV)	Area	Line shape	BE (eV)	FWHM (eV)	Area
Na1s	Na0	1071.56	0.66	160516	LF(0.58,1.17,200,85)	-	0.6 - 0.75	-
	Surf. plasmon	1075.38	1.84	97758	//	1075.2 - 1075.6	1.6 - 2	-
	Bulk plasmon	1077.37	1.13	75114	//	1077 - 1079	0.8 - 1.2	-
	NZSP	1073.47	1.45	55030	LA(1.53,243)	1073.2 - 1073.8	1.45 - 1.65	Fixed - same Na:Si ratio as ref. sample
	int. & pass.	1073.05	1.97	136388	LA(1.53,243)	-	-	-
P2p	3/2 NZSP	135.09	1.27	1018	LA(1.53,243)	-	-	-
	1/2 NZSP	135.96	1.27	509	LA(1.53,243)	P2p3/2 + 0.87	P2p3/2 *1	P2p3/2*0.5
Si2p	3/2 NZSP	103.55	1.51	858	LA(1.53,243)	-	-	-
	1/2 NZSP	104.15	1.51	429	LA(1.53,243)	Si2p3/2 +0.6	Si2p3/2*1	Si2p3/2*0.5
Zr3d	5/2 NZSP	184.55	1.50	3246	LA(1.53,243)	184 -184.55	1 - 1.5	-
	3/2 NZSP	186.95	1.50	2164	LA(1.53,243)	Zr3d5/2 (NZSP) + 2.4	Zr3d5/2 (NZSP)*1	Zr3d5/2 (NZSP)*0.667
	5/2 int. 1	183.66	1.50	2159	LA(1.53,243)	183 -183.7	Zr3d5/2 (NZSP)*1	-
	3/2 int. 1	186.06	1.50	1439.02	LA(1.53,243)	Zr3d5/2 (SEI1) + 2.4	Zr3d5/2 (NZSP)*1	Zr3d5/2 (SEI1)*0.667
	5/2 int. 2	182.24	1.50	434.607	LA(1.53,243)	181 - 183	Zr3d5/2 (NZSP)*1	-
	3/2 int. 2	184.64	1.50	289.738	LA(1.53,243)	Zr3d5/2 (SEI2) + 2.4	Zr3d5/2 (NZSP)*1	Zr3d5/2 (SEI2)*0.667

Background:

- the Na1s region was fitted with a Tougaard background (U 4 Tougaard: 0.8, 33, 0.8, 0). The first cross-section term (which modulates the intensity of the background) was optimized for each plating cycle to minimize residuals
- all other peaks were fitted with a Shirley type background

Table S3 – XPS fitting parameters of the Na^0|$NZSP_{polished}$ interface (dataset collected after 91 minutes of plating). Related to Figure 3.

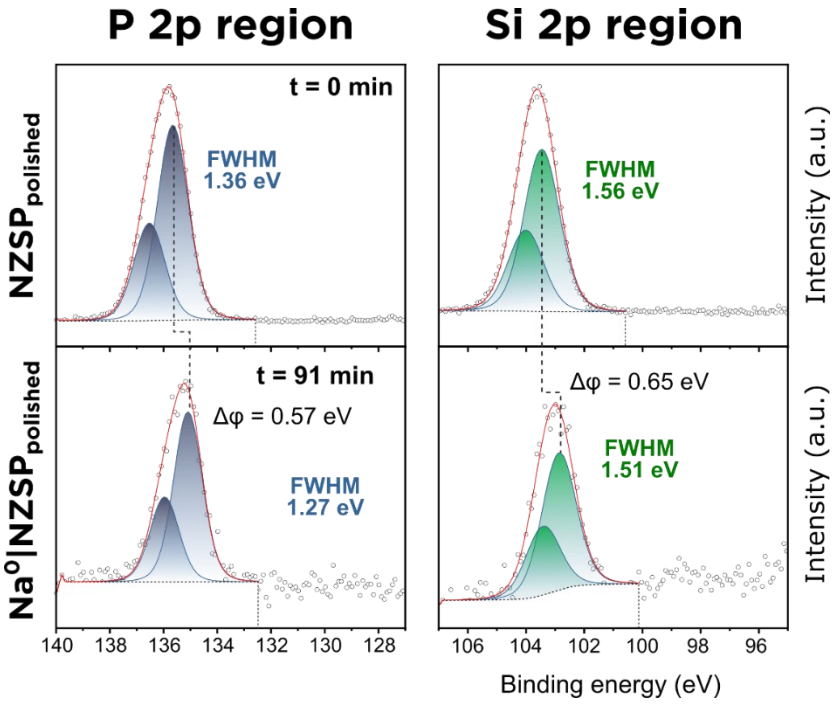

Figure S3 – The P2p and Si2p core level regions of the $Na^0|NZSP_{polished}$ interface compared with those of the reference $NZSP_{polished}$ sample.

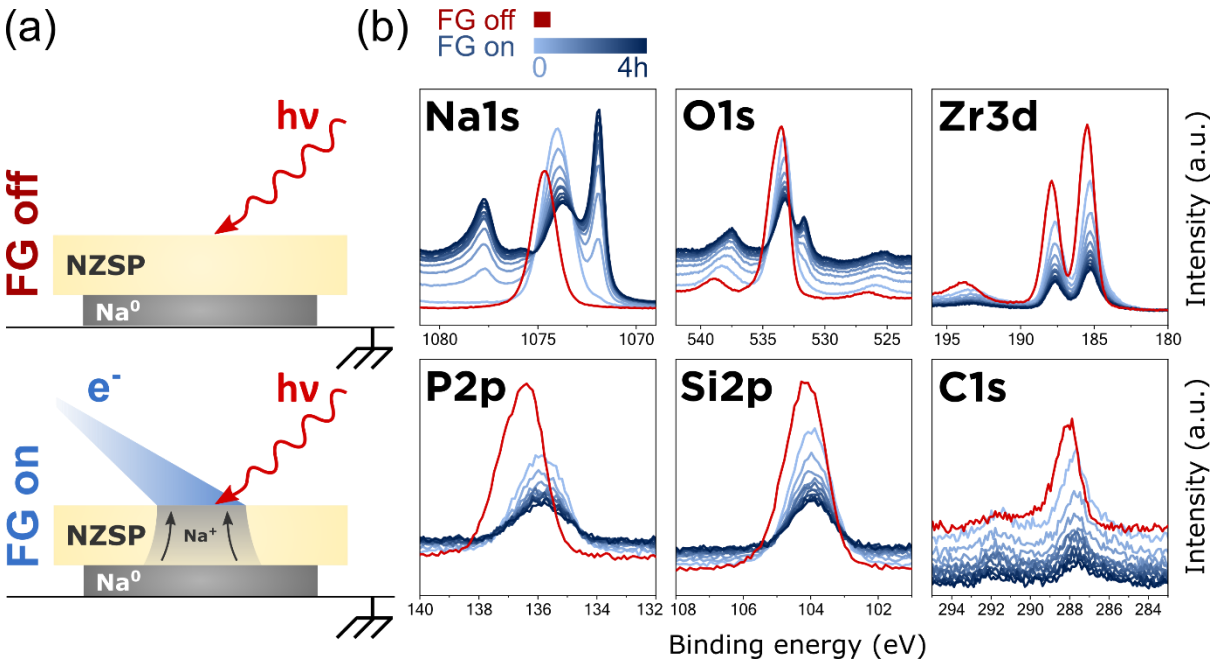

Figure S4 – *Operando* plating of Na^0 on a $NZSP_{AS}$ surface inside the XPS. (a) Schematic representation of the two XPS analysis configurations; (b) Evolution of selected core level regions with increasing Na^0 plating time. An initial set of data (in red) was measured with the FG off (reference signal from $NZSP_{AS}$). The following spectra (in shades of blue) were measured in an iterative loop (each iteration lasted 33 minutes).

		Fitting			Constraints			
Region	Peak	BE (eV)	FWHM (eV)	Area	Line shape	BE (eV)	FWHM (eV)	Area
Na1s	NZSP	1074.63	1.4	166765	LA(1.15,1.4,243)	-	-	-
P2p	3/2 NZSP	136.29	1.31	3830	LA(1.53,243)	-	-	-
	1/2 NZSP	135.96	1.31	1915	//	P2p3/2 + 0.87	P2p3/2 *1	P2p3/2*0.5
Si2p	3/2 NZSP	103.55	1.19	3659	LA(1.53,243)	-	-	-
	1/2 NZSP	104.15	1.19	1829	//	Si2p3/2 +0.6	Si2p3/2*1	Si2p3/2*0.5
Zr3d	5/2 NZSP	184.55	1.24	25307	LA(1.53,243)	-	-	-
	3/2 NZSP	186.95	1.24	16872	//	Zr3d5/2 (NZSP) + 2.4	Zr3d5/2 (NZSP)*1	Zr3d5/2 (NZSP)*0.667

Table S4 – XPS fitting parameters of the reference $NZSP_{AS}$ sample. Related to Figure 4.

		Fitting			Constraints			
Region	Peak	BE (eV)	FWHM (eV)	Area	Line shape	BE (eV)	FWHM (eV)	Area
Na1s	Na0	1071.88	0.65	91680	LF(0.58,1.17,200,80)	-	0.65	-
	Surf. plasmon	1075.84	1.79	46109	//	-	-	-
	bulk plasmon	1077.7	1.03	28614	//	1077-1080	-	-
	NZSP	1073.83	1.8	44400	LA(1.53,243)	-	-	Fixed - same Na:Si ratio as ref. sample
	int. & pass.	1075.58	1.78	6502	//	1072-1073.8	-	-
P2p	3/2 NZSP	135.6	1.54	1020	LA(1.53,243)	-	-	-
	1/2 NZSP	136.47	1.54	510	//	P2p3/2 + 0.87	P2p3/2 *1	P2p3/2*0.5
Si2p	3/2 NZSP	103.81	1.14	1063	LA(1.53,243)	-	-	-
	1/2 NZSP	104.41	1.14	531.5	//	Si2p3/2 +0.6	Si2p3/2*1	Si2p3/2*0.5
Zr3d	5/2 NZSP	185.27	1.21	6001	LA(1.53,243)	-	-	-
	3/2 NZSP	187.67	1.21	4000.6	//	Zr3d5/2 (NZSP) + 2.4	Zr3d5/2 (NZSP)*1	Zr3d5/2 (NZSP)*0.667
	5/2 int. 1	184.05	1.21	923	//	-	Zr3d5/2 (NZSP)*1	-
	3/2 int. 1	186.45	1.21	615.6	//	Zr3d5/2 (SEI1) + 2.4	Zr3d5/2 (NZSP)*1	Zr3d5/2 (SEI1)*0.667
	5/2 int. 2	182.7	1.21	270.3	//	-	Zr3d5/2 (NZSP)*1	-
	3/2 int. 2	185.1	1.21	180.21	//	Zr3d5/2 (SEI2) + 2.4	Zr3d5/2 (NZSP)*1	Zr3d5/2 (SEI2)*0.667
Background: - the Na1s region was fitted with a Tougaard background (U 4 Tougaard: 1.45, 33, 0.8, 0). The first cross-section term (which modulates the intensity of the background) was optimized for each plating cycle to minimize residuals - all other peaks were fitted with a Shirley type background								

Table S5 – XPS fitting parameters of the Na^0|$NZSP_{AS}$ interface (dataset collected after 240 minutes of plating). Related to Figure 4.

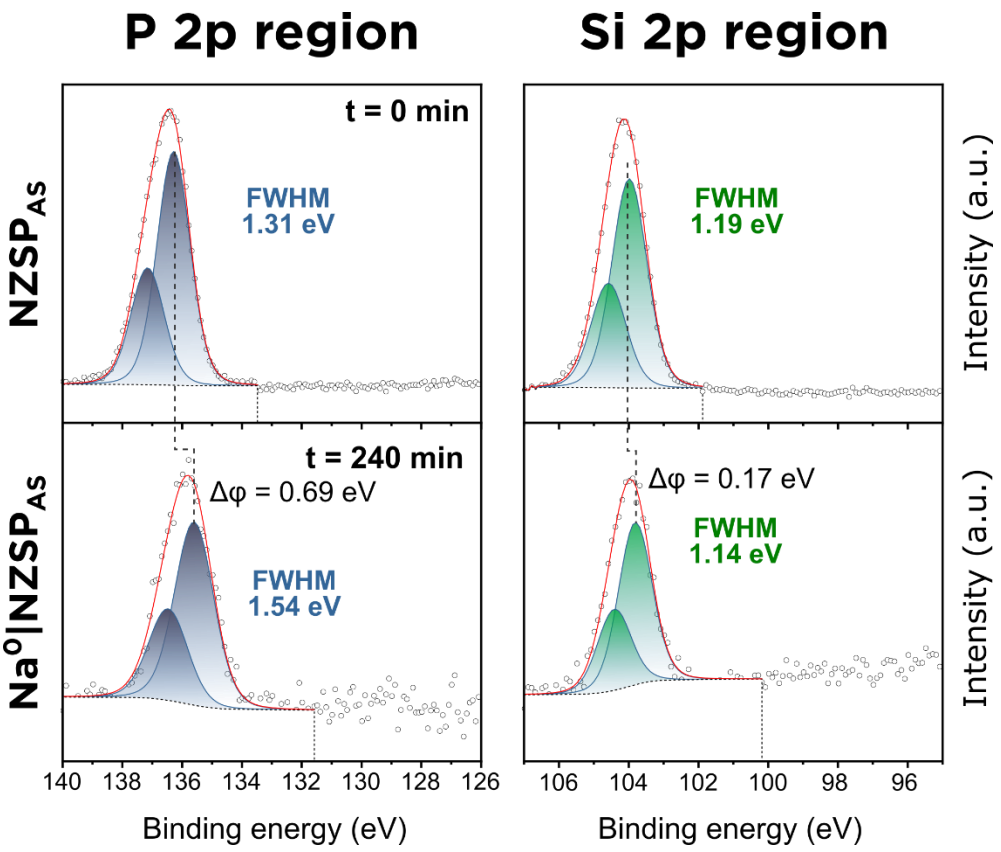

Figure S5 – The P2p and Si2p core level regions of the Na^0|$NZSP_{AS}$ interface compared with those of the reference $NZSP_{AS}$ sample.

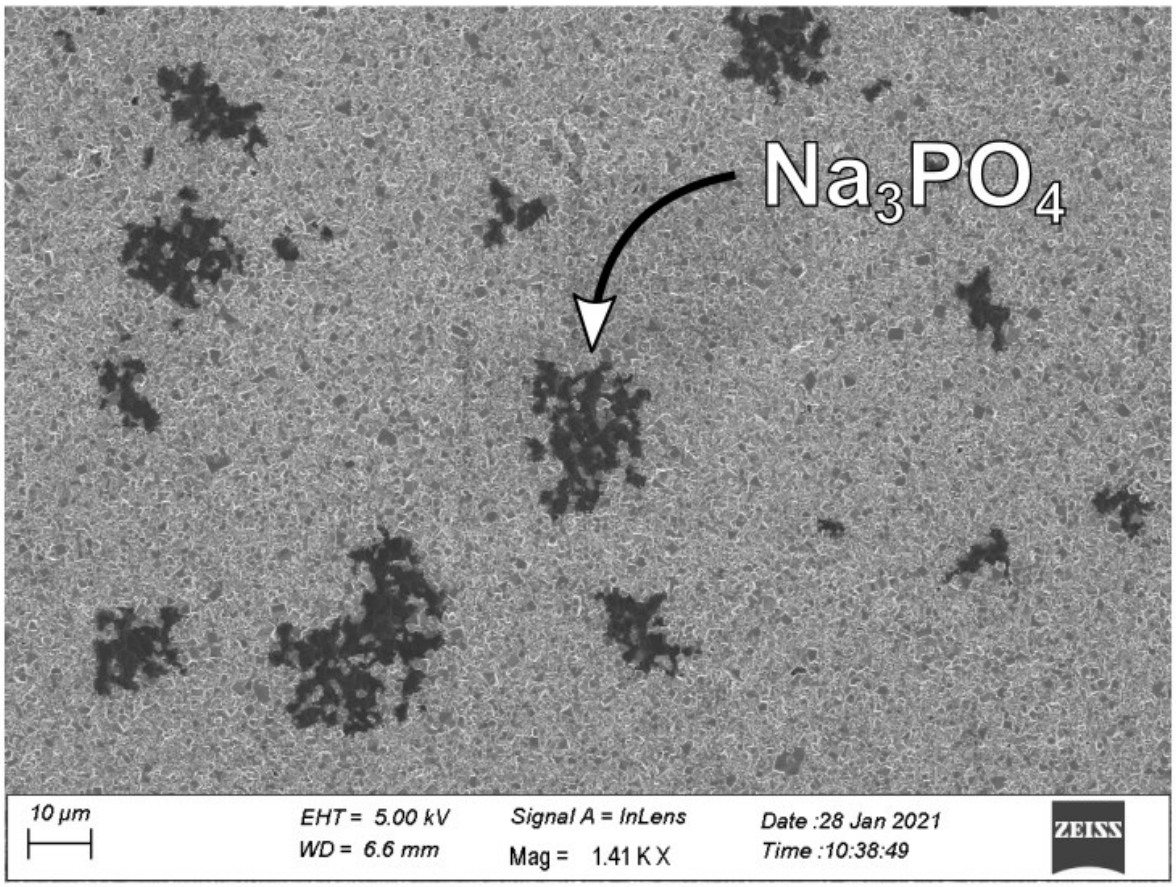

Figure S6 – SEM micrograph of a $NZSP_{AS}$ surface collected in secondary electron mode using the in-lens detector of a Zeiss Leo Gemini 1525 at a working distance of 7 mm with an electron beam accelerating voltage of 5 kV and a 30 µm aperture. The composition of the darker islands was identified to be a sodium phosphate phase by EDX in a previous study.[3] Related to Figure 6.

References

1. Jain, A. *et al.* Commentary: The materials project: A materials genome approach to accelerating materials innovation. *APL Materials* **1**, 011002 (2013).
2. Wood, K. N. & Teeter, G. XPS on Li-Battery-Related Compounds: Analysis of Inorganic SEI Phases and a Methodology for Charge Correction. *ACS Appl. Energy Mater.* **1**, 4493–4504 (2018).
3. Querel, E. *et al.* The role of NaSICON surface chemistry in stabilizing fast-charging Na metal solid-state batteries. *J. Phys. Energy* **3**, (2021).